Simulation of Weather-Driven Deterioration of Clay Embankments

Amr M. Morsy, Ph.D., P.E., M.ASCE[1]; Peter R. Helm, Ph.D.[2];
Ashraf El-Hamalawi, Ph.D., P.E., M.ASCE[3]; Alister Smith, Ph.D., CEng[4];
and Ross A. Stirling, Ph.D.[5]

[1]Dept. of Civil Engineering and Construction Engineering Management, California State Univ. Long Beach, Long Beach, CA. Email: amr.morsy@csulb.edu
[2]School of Engineering, Newcastle Univ., Newcastle upon Tyne, England, UK. Email: peter.helm@newcastle.ac.uk
[3]School of Architecture, Building, and Civil Engineering, Loughborough Univ., Loughborough, England, UK. Email: a.el-hamalawi@lboro.ac.uk
[4]School of Architecture, Building, and Civil Engineering, Loughborough Univ., Loughborough, England, UK. Email: a.smith10@lboro.ac.uk
[5]School of Engineering, Newcastle Univ., Newcastle upon Tyne, England, UK. Email: ross.stirling@newcastle.ac.uk

ABSTRACT

Clay embankments used for road, rail, and flood defense infrastructure experience several weather-driven deterioration processes that lead to a progressive degradation in their hydromechanical performance. This paper presents a numerical modeling approach that accounts for the development of desiccation cracking in clay embankments. Specifically, a bimodal soil-water retentivity model was adopted to capture the long-term hydraulic behavior of clay embankments prone to weather-driven desiccation cracking. A numerical model was developed for a heavily instrumented and monitored full-scale research embankment with long-term field data. The model was able to capture the variation of near-surface soil moisture and matric suction over a monitored period of nine years in response to weather cycles. The developed and validated numerical modeling approach enables forecasting of the long-term performance of clay embankments under a range of future climate scenarios.

INTRODUCTION

Significant embankment construction in the UK and around the world has been undertaken since the 1800s (Trenter 2001) to support infrastructure such as railroads, highways, and flood defense embankments. Unexpected failures of these embankments have severe societal and economic consequences, including fatalities. The performance of infrastructure assets supported by embankments is affected by time-dependent deterioration processes of soils. It is evident that weather-driven deterioration mechanisms contribute significantly to the overall deterioration of earth infrastructure assets, where weather cycles can lead to progressive failure (*e.g.*, Templeton *et al.* 1984; Vaughan *et al.* 2004; Rouainia *et al.* 2009; Kovacevic *et al.* 2013). Weather-related deterioration mechanisms adversely affect soil hydromechanical behavior through strength reduction (Skempton 1964), desiccation cracking (Anderson et al. 1982; Cheng et al. 2020), downslope ratcheting (Take and Bolton 2011; Lees et al. 2013), softening of clay lumps during wet seasons (Skempton 1996), and reorientation of clay particles (Kayyal and Wright 1991).

While significant advances have been made in the understanding of element- and asset-scale deterioration of earthworks infrastructure, further investigations and analyses of slope failures are needed for improved asset management (*e.g.*, Network Rail 2021). Current practice requires enhanced capabilities to forecast future performance and the remaining service life of aging infrastructure in the form of robust and reliable modeling approaches that can take account of weather-driven deterioration mechanisms. This paper presents a numerical modeling approach that accounts for the development of desiccation cracking in clay embankments. Specifically, a bimodal soil-water retentivity model was adopted to capture the long-term hydraulic behavior of clay embankments prone to weather-driven desiccation cracking. A numerical model was developed for a heavily instrumented and monitored full-scale research embankment with long-term field data. The model was able to capture the variation of near-surface soil moisture and matric suction over a monitored period of nine years in response to weather cycles. The developed and validated numerical modeling approach enables forecasting of the long-term performance of clay embankments under a range of future climate scenarios.

BIONICS RESEARCH EMBANKMENT

A purpose-built research embankment was constructed in 2005 to allow full-scale field experiments on soil-atmosphere interaction (Hughes *et al.* 2009) as part of the UK biological and engineering impacts of climate change on slopes (BIONICS) project. The embankment was constructed near Stocksfield, Northumberland, United Kingdom. The embankment is 90 m in length with 5 m crest width, 6 m height, and 2H:1V side slopes, as depicted in Figure 1. The embankment was heavily instrumented with conjugate moisture content and matric suction sensors and has been monitored since December 2008 (approximately 3 years since end of construction in November 2005). The monitoring data used in the present study include water content and matric suction time series from instrumentation placed at depths 0.5 and 1.0 m, and at 3 and 9 m from the embankment toe, as shown in Figure 1. The matric suction was measured using dielectric water potential sensors, which can measure matric suction in the range of −10 to −500 kPa.

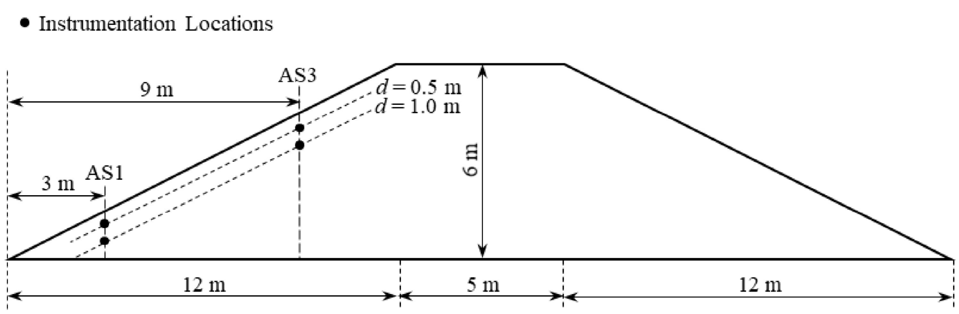

Figure 1. Cross-section of the BIONICS research embankment showing instrumentation depths at AS1 and AS3 locations (adapted from Hughes *et al.* 2009).

EMBANKMENT NUMERICAL MODEL

FLAC (Fast Lagrangian Analysis of Continua) software v8.1 (Itasca 2016) was used to develop a multi-phase hydromechanical numerical model for the BIONICS research embankment. The software allows the performance of coupled multi-phase hydromechanical analyses that can be defined by user subroutines, which were developed to allow transient calculations of coupled hydromechanical behavior.

Boundary conditions. The modeling was undertaken using a two-dimensional plane strain analysis and one-half of the BIONICS symmetric embankment was modeled. The bottom boundary was constrained in both the horizontal and vertical directions. The lateral boundaries were constrained from displacement in the horizontal direction and were free to displace in the vertical direction. The thickness of the foundation layer in the model was selected to be twice the slope height from the embankment base, and its lateral extent was selected to be four times the slope height, as shown in Figure 2. The initial groundwater elevation was specified at a depth of 6 m below the embankment base. Flow was restricted through the model side and bottom boundaries. However, these boundaries allow for free saturation and pore pressure changes over time.

A transient climate boundary was defined at the surface of the model to simulate soil-atmosphere interaction. The climate boundary calculates the daily surface net flux, q_{nf}, as the difference between precipitation, P, and actual evapotranspiration, ET_a, A weather station was installed at the embankment site (Hughes *et al.* 2009), which measured weather parameters and was used to produce time histories to estimate reference evapotranspiration, ET_0, using the Penman-Monteith method as adopted by FAO56 (Allen *et al.* 1998) for reference grass, which was factored by a daily average crop coefficient, K_c, to account for the typical grass at the BIONICS embankment and its typical seasonal variation. The daily q_{nf} values were divided uniformly over 24 hours and input in the climate boundary subroutine at every surface mesh node as it executed every one simulation hour to determine a boundary flux, Q, based on each node's pore pressure condition. The pore-air pressure, u_a, was set and fixed at zero (atmospheric gauge pressure) at the ground surface (see details of climate boundary in Morsy *et al.* 2023a).

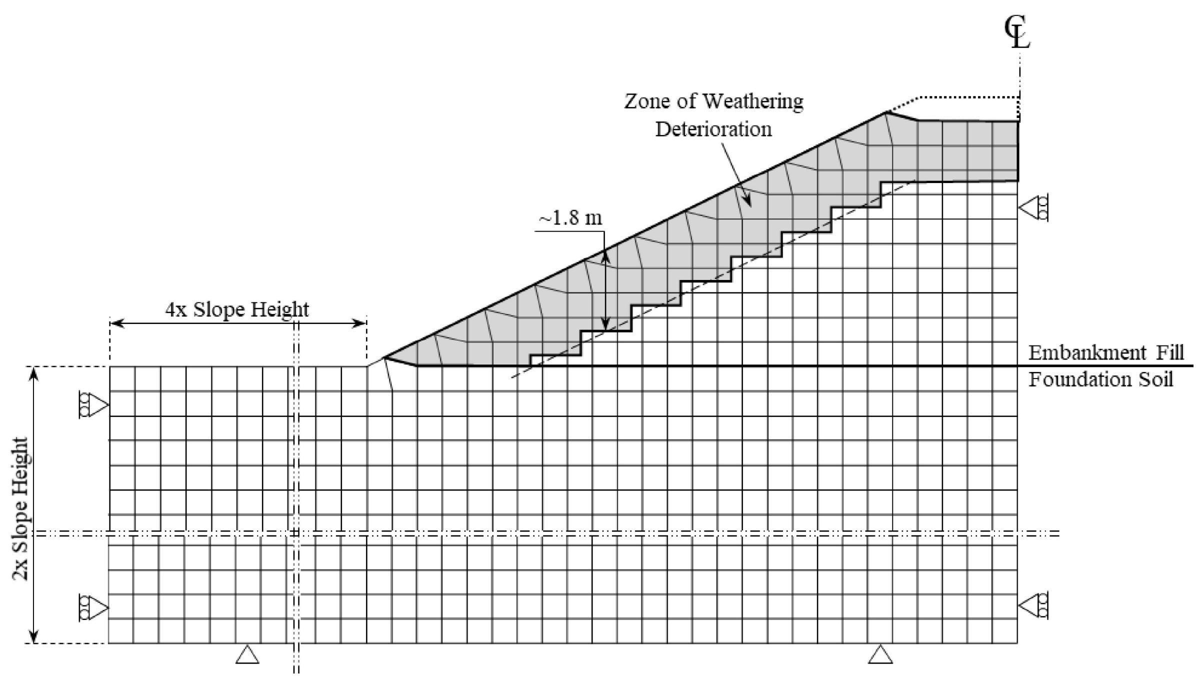

Figure 2. Finite-difference mesh used to model the BIONICS research embankment (after Morsy *et al.* 2023a).

Hydraulic model. Fluid transport is described in FLAC by Darcy's law (Itasca 2016). The soil-water retention curves were developed based on field measurements and were represented using the van Genuchten (1980) fitting model for both the embankment fill and the foundation soil, as follows:

$$\psi_m = u_a - u_w = \psi_{m,o}\left({S_e}^{-1/a_{vg}} - 1\right)^{1-a_{vg}} \tag{1}$$

where, ψ_m is the matric suction (*i.e.*, the difference between the pore-air, u_a, and pore-water, u_w, pressures), $\psi_{m,o}$ is a fitting parameter that can be related to the matric suction at air entry, a_{vg} is a fitting parameter, and S_e is the effective saturation, which can be expressed as $S_e = \frac{S_w - S_{w,r}}{1 - S_{w,r}}$, where S_w is the degree of water saturation and $S_{w,r}$ is the residual degree of water saturation. The pore fluids were treated as two immiscible fluids that can only displace each other within the void volume. That is, the degree of gas saturation can be expressed in terms of the degree of water saturation as $S_g = 1 - S_w$, where S_g is the degree of gas saturation.

The hydraulic conductivity functions were correlated to the soil-water retention curves using the van Genuchten-Mualem model (Mualem 1976; van Genuchten 1980) as $k_w = \kappa_{r,w} \,.\, k_{w,sat}$, where k_w is the hydraulic conductivity, $k_{w,sat}$ is k_w at 100% water saturation, and $\kappa_{r,w}$ is the relative hydraulic conductivity, which can be expressed as follows:

$$\kappa_{r,w} = {S_e}^{b_{vg}}[1 - (1 - {S_e}^{1/a_{vg}})^{a_{vg}}]^2 \tag{2}$$

where, b_{vg} is a fitting parameter. The air conductivity functions were correlated to those of the hydraulic conductivity (Itasca 2016) as $k_g = \kappa_{r,g} \,.\, k_{g,sat}$, where k_g is the gas conductivity, and $k_{g,sat}$ is k_g at 100% water saturation, which was derived from the saturated hydraulic conductivity and the water-to-air dynamic viscosity ratio, μ_r, as $k_{g,sat} = \gamma_g \,.\, \mu_r \,.\, k_{w,sat}$, and $\kappa_{r,g}$ is the relative gas conductivity, which can be expressed as follows:

$$\kappa_{r,g} = (1 - S_e)^{c_{vg}}(1 - {S_e}^{1/a_{vg}})^{2a_{vg}} \tag{3}$$

where, c_{vg} is a fitting parameter. The saturated hydraulic conductivity, $k_{w,sat}$, was correlated to the void ratio, e, according to the empirical formula proposed by Samarasinghe *et al.* (1982) as $k_{w,sat} = C\left(\frac{e^l}{1+e}\right)$, where C and l are empirical constants that are specific for soil mineralogy (Mesri and Olson 1971; Samarasinghe *et al.* 1982). The empirical constants, C and l, were selected based on the field data reported by Dixon *et al.* (2019) for the BIONICS embankment and for the range of void ratios deduced from the volumetric water content field data during wet seasons and compaction data. The same hydraulic models were adopted for the foundation soil. The parameters of the hydraulic models are summarized in Table 1.

Weathering of near-surface soils occurs because of cyclic wetting and drying that introduce near-surface cracking and clay aggregation. This can change the pore network and in turn the hydraulic behavior of soils from their behavior when originally intact. Specifically, the soil water retentivity and hydraulic conductivity can evolve into bimodal forms as the global porosity and saturated conductivity increase (Li *et al.* 2011; Fredlund *et al.* 2012). Based on the field monitoring data from the BIONICS embankment, recorded using conjugate soil moisture and matric suction sensors, at various near-surface locations and during several seasonal cycles of wetting and drying, it was observed that the soil-water retention data (volumetric water content, θ, versus matric suction, ψ) exhibit obvious bimodality. To account for this bimodality in the numerical model, near-surface soils were simulated using a bimodal soil-water retention curve and fluid conductivity functions, as shown schematically in Figures 3a and 3b, respectively.

Table 1. Soil hydraulic parameters (after Morsy *et al.* 2023a).

Parameter	Value
Soil-Water Retention Model Fitting Parameter, α_{vg} (-)	0.25
Hydraulic Conductivity Function Fitting Parameter, b_{vg} (-)	0.50
Gas Conductivity Function Fitting Parameter, c_{vg} (-)	0.50
Soil-Water Retention Model Fitting Parameter, $\psi_{m,o}$ (kPa)	80.00
Residual Degree of Water Saturation, $S_{w,r}$ (-)	0.00
Water-To-Air Dynamic Viscosity Ratio, μ_r (-)	55.00
Hydraulic conductivity empirical constant, C (m/s)	1.00×10^{-6}
Hydraulic conductivity empirical constant, l (-)	5.00

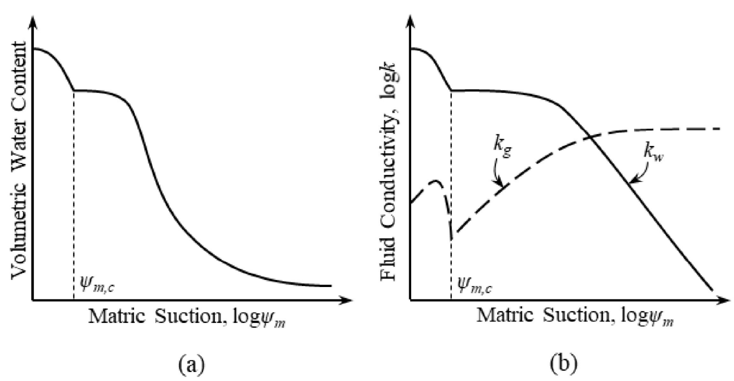

Figure 3. Representation of bimodal soil-water retention curve and fluid conductivity functions for weathered soils: (a) retention curve; and (b) conductivity functions (after Morsy *et al.* 2023a).

Based on the field measurements of soil moisture and matric suction, the increase in moisture content during wet periods was approximately 15%. Additionally, field measurements of desiccation cracks collected at the BIONICS embankment for a complete year (Yu *et al.* 2020) were used to estimate the volume of cracks, and the corresponding increase in global porosity as $n_c = n_i + \frac{V_c}{d_c\, S_c^2}$, where n_c is the global porosity of the desiccated soil, n_i is the porosity of the intact soil, V_c is the average volume of a unit crack, d_c is the average crack depth, and S_c is the average tributary spacing for a unit crack, as shown in Figure 4. Desiccation cracking can be quite complex to idealize; however, cracks have usually been described by the relationship between their spacings and depths, where the ratio between crack spacing to crack depth is unity (Chertkov 2000; Aubeny and Lytton 2004). Figure 4 shows data for crack spacings and depths for six clay types (Zein el Abedine and Robinson 1971; Yaalon and Kalmar 1984; Dasog *et al.* 1987), which suggest that a relationship crack spacing of 1.2 times the crack depth serve as a reasonable simplification.

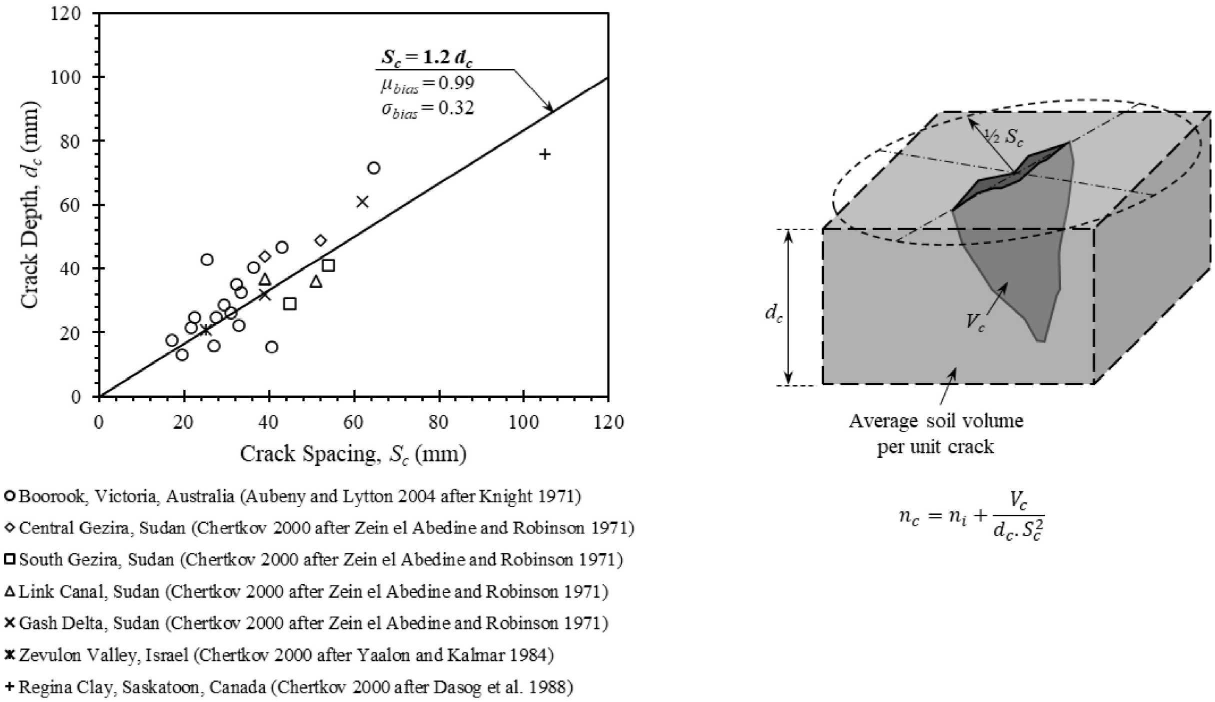

Figure 4. Field measurements of crack spacings and corresponding depths compiled from literature. The compiled data was used to develop the relationship between crack spacing and depth used in this study. On the right-hand side is a schematic showing a crack and a tributary volume for a unit crack in a crack network.

Figures 5a and 5b replot the crack volume and crack depth data, respectively, by Yu *et al.* (2020) normalized to their maximum values. As shown in the figures, the cracks open to their maximum size in September through October and close to their minimum size during March through June. Based on the data shown in Figure 5, the annual average volume of cracks was estimated to be approximately 40% of the maximum volume (*i.e.*, area under the idealized black line in Figure 5a divided by 365 days). Knowing the average maximum crack depth, d_c, and the annual average crack volume, V_c, the increase in global porosity of the near-surface weathered soil zone could be estimated to be approximately 15%, which agrees with field observations.

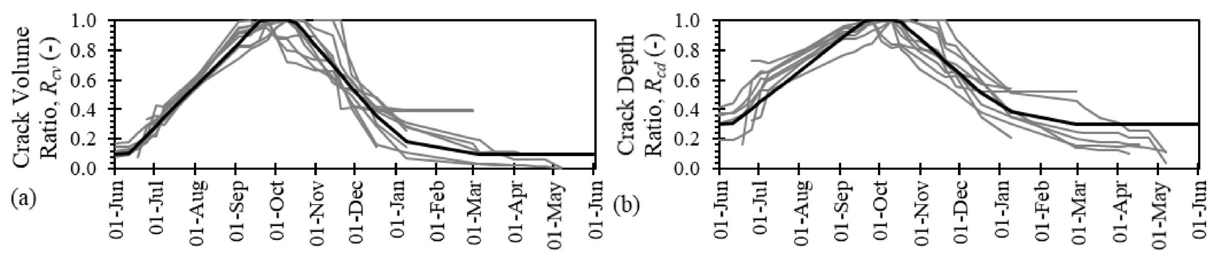

Figure 5. Seasonal variation of major shrinkage crack (a) volume and (d) depth of the embankment fill. Absolute data were obtained from Yu *et al.* (2020) database for the embankment case study. The data were used to estimate the volume of cracks. R_{cv} is the ratio of crack volume to maximum volume at maximum shrinkage, and R_{cd} is the ratio of crack depth to maximum depth at maximum shrinkage.

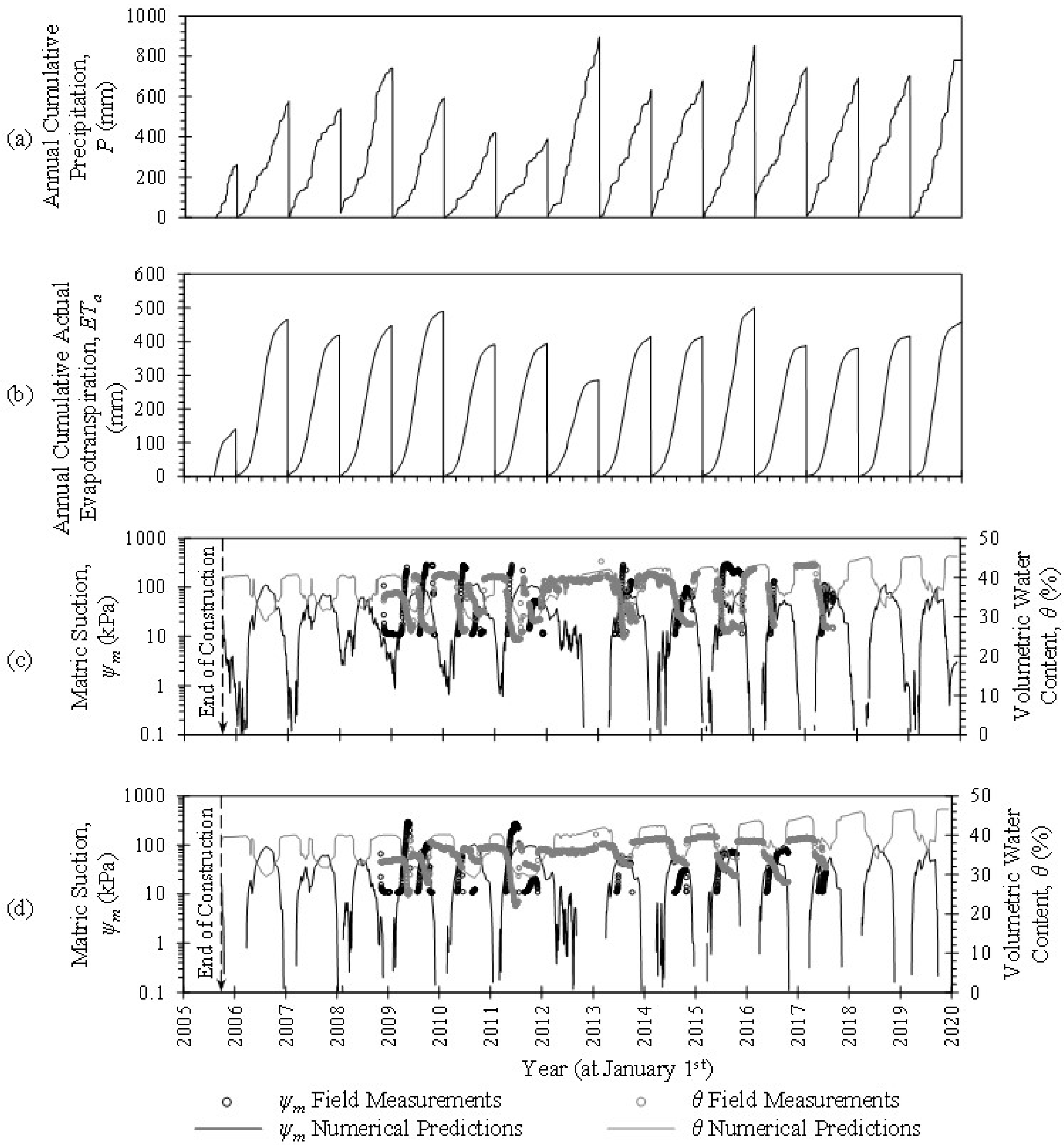

Figure 6. Weather data, field measurements and numerical predictions of soil matric suction and volumetric water content at the BIONICS embankment: (a) annual cumulative precipitation, *P*; and (b) annual cumulative actual evapotranspiration, ET_a; (c) soil matric suction and volumetric water content at AS1 and depth 0.5 m; and (d) soil matric suction and volumetric water content at AS1 and depth 1.0 m (adapted from Morsy *et al.* 2023a).

RESULTS AND DISCUSSIONS

To evaluate the performance of the developed numerical model in predicting the hydraulic response of the BIONICS embankment, model predictions were compared to the field monitoring data collected from December 2008 through August 2017 (Yu *et al.* 2021). Data from conjugate moisture content and matric suction sensors located at AS1 (see Figure 1) at depths 0.5 and 1.0 m below the ground surface were curated and used in this comparison. Figure 6 shows that the numerical model predictions and field measurements were comparable in magnitude and distribution with time, including during wet seasons when bimodality of soil hydraulic behavior dominates. Additionally, the model could capture the prolonged wet period observed in the field data from mid-2011 through mid-2013 (see Figure 6). These results demonstrate that the numerical modeling approach was able to replicate real, long-term hydraulic behavior. Specifically, the variation of the soil-fluid retentivity and fluid conductivity functions in response to soil volumetric changes captured the range of soil water retention data observed in the field data despite the absence of field monitored volumetric strain data. For instance, it was evident from the field data that volumetric water contents during wet season increase every year compared to the preceding years (see Figure 6), indicating an irrecoverable increase in volume (due to increase soil porosity) after every seasonal shrink-swell cycle. This increase in volume and volumetric water content with time was captured by the model (see Figure 6). Additionally, the bimodality of the soil-fluid retentivity and fluid conductivity functions could capture the continued increase in moisture beyond the initial saturated water content (equivalent to initial soil porosity) for non-weathered soil during the wet seasons. Finally, the model was able to vary the hydraulic conductivity with depth seasonally and over the monitored period, where the hydraulic conductivity increases near surface as a result of the seasonal increase in volume (introduced by the bimodality in the fluid conductivity functions), as well as the irrecoverable increase in volume after shrink-swell cycles. This variation of the hydraulic conductivity with depth was reported to develop near surface due to weathering (*e.g.*, Dixon *et al.* 2019), which was incorporated in the model allowing for the variation to develop during the simulation.

CONCLUSIONS

This study has developed a numerical modeling approach to simulate the construction and long-term, weather-driven hydromechanical behavior of clay embankments. Subroutines were developed to capture a suite of deterioration processes and achieve a hydromechanical coupling that allowed matric suction, water content, and void ratio to change interactively. Capturing these deterioration processes is unique to the model approach developed in this study. The numerical modeling approach was comprehensively validated by comparing predicted hydromechanical behavior with laboratory tests, results from the literature, and nine years of measurements from a full-scale, purpose-built research embankment, namely BIONICS research embankment. For the embankment case study, the hydraulic response was validated through model prediction and field measurement comparisons of near-surface soil moisture and matric suction. This emphasizes the importance of high-quality, long-term field monitoring data for validating numerical models and to better understand changes in behavior over time. Overall, the presented numerical modeling approach enables forecasting of the long-term performance of clay embankments.

ACKNOWLEDGEMENTS

The work presented in this paper was conducted as part of the ACHILLES program grant (EP/R034575/1) funded by the Engineering and Physical Sciences Research Council (EPSRC). Some of the field and laboratory data used in this study were obtained as part of the BIONICS project (GR/S87430/01) and the iSMART project (EP/K027050/1) both funded by the EPSRC. Amr Morsy acknowledges the support of the California State University Transportation Consortium through its TRANSPORT grant (G2738-G27382310F). The opinions presented in this paper are those of the authors and are not necessarily those of the funding entities.

REFERENCES

Allen, R. G., Pereira, L. S., Raes, D., and Smith, M. (1998). Crop evapotranspiration-Guidelines for computing crop water requirements-FAO Irrigation and drainage paper 56. *FAO, Rome*, 300(9), D05109.

Anderson, M. G., Hubbard, M. G., and Kneale, P. E. (1982). "The influence of shrinkage cracks on pore-water pressures within a clay embankment." *Q. Journal of Eng. Geology & Hydrogeol*, 15(1):9-14.

Aubeny, C. P., and Lytton, R. L. (2004). "Shallow slides in compacted high plasticity clay slopes." *Journal of Geotechnical and Geoenvironmental Engineering*, 130(7):717-727.

Cheng, Q., Tang, C. S., Zeng, H., Zhu, C., An, N., and Shi, B. (2020). "Effects of microstructure on desiccation cracking of a compacted soil." *Engineering Geology*, 265, 105418.

Chertkov, V. Y. (2000). "Using surface crack spacing to predict crack network geometry in swelling soils." *Soil Science Society of America Journal*, 64 (6):1918-1921.

Dasog, G. S., Acton, D. F., Mermut, A. R., and DeJong, E. (1988). "Shrink-swell potential and cracking in clay soils of Saskatchewan." *Canadian Journal of Soil Science*, 68(2):251-260.

Dixon, N., et al. (2019). "In situ measurements of near-surface hydraulic conductivity in engineered clay slopes." *Quarterly Journal of Engineering Geology & Hydrogeology*, 52(1):123-135.

Fredlund, D. G., Rahardjo, H., and Fredlund, M. D. (2012). *Unsaturated Soil Mechanics in Engineering Practice*. John Wiley & Sons, Inc., Hoboken, New Jersey, US, 926p.

Hughes, P. N., et al. (2009). "Full-scale testing to assess climate effects on embankments." *Proc. of the Institution of Civil Engineers-Engineering Sustainability*, 162(2):67-79.

Itasca. (2016). *Fast Lagrangian Analysis of Continua V. 8.0 – User's Guide*. 6th edition, Itasca Consulting Group Inc., Minneapolis, US.

Kayyal, M. K., and Wright, S. G. (1991). Investigation of long-term strength properties of Paris and Beaumont clays in earth embankments. Report FHWA/TX-92+1195-2F, Center for Transportation Research, Austin, TX.

Kovacevic, N., Hight, D. W., Potts, D. M., and Carter, I. C. (2013). "Finite-element analysis of the failure and reconstruction of the main dam embankment at Abberton Reservoir, Essex, UK." *Géotechnique*, 63(9):753-767.

Lees, A. S., MacDonald, G. J., Sheerman-Chase, A., and Schmidt, F. (2013). "Seasonal slope movements in an old clay fill embankment dam." *Canadian Geotechnical Journal*, 50(5):503-520.

Li, J. H., Zhang, L. M., and Li, X. (2011). "Soil-water characteristic curve and permeability function for unsaturated cracked soil." *Canadian Geotechnical Journal*, 48(7):1010-1031.

Mesri, G., and Olson, R. E. (1971). "Mechanisms controlling the permeability of clays." *Clays*

Morsy, A. M., Helm, P. R., El-Hamalawi, A., Smith, A., Hughes, P. N., Stirling, R. A., Dijkstra, T. A., Dixon, N., and Glendinning, S. (2023a). "Development of a Multi-Phase Numerical Modeling Approach for Hydromechanical Behavior of Clay Embankments Subject to Weather-Driven Deterioration," *Journal of Geotechnical and Geoenvironmental Engineering*, 149(8): 04023062.

Morsy, A. M., Helm, P. R., El-Hamalawi, A., Smith, A., Hughes, P. N., Stirling, R. A., Dijkstra, T. A., Dixon, N., and Glendinning, S. (2023b). Data Used for the Validation of the BIONICS Research Embankment Hydromechanical Model. Dataset, Newcastle University.

Mualem, Y. (1976). "A new model for predicting the hydraulic conductivity of unsaturated porous media." *Water Resources Research*, 12(3):513-522.

Network Rail. (2021). A review of earthworks management. Prepared by a Task Force led by Professor Lord Robert Mair, Milton Keynes, UK, February 2021.

Rouainia, M., Davies, O., O'Brien, T., and Glendinning, S. (2009). "Numerical modelling of climate effects on slope stability." *Proc. of Institution of Civil Engineers-Eng.Sustainability*, 162(2), pp. 81-89.

Samarasinghe, A. M., Huang, Y. H., and Drnevich, V. P. (1982). "Permeability and consolidation of normally consolidated soils." *J. of the Geotechnical Engineering Division*, 108(6): 835-850.

Skempton, A. W. (1964). "Long-term stability of clay slopes." *Géotechnique*, 14(2): 77-102.

Skempton, A. W. (1996). "Embankments and cuttings on the early railways." *Const History*, 11, pp. 33-49.

Take, W. A., and Bolton, M. D. (2011). "Seasonal ratcheting and softening in clay slopes, leading to first-time failure." *Géotechnique*, 61(9):757-769.

Templeton, A. E., Sills, G. L., and Cooley, L. A. (1984). "Long term failure in compacted clay slopes." In *Proc. of International Conference on Case Histories in Geotechnical Engineering*, 749-754.

Trenter, N. A. (2001). *Earthworks: A Guide*. Thomas Telford Ltd, London.

van Genuchten, M. T. (1980). "A closed-form equation for predicting the hydraulic conductivity of unsaturated soils." *Soil Science Society of America Journal*, 44(5):892-898.

Vaughan, P. R., Kovacevic, N., and Potts, D. M. (2004). "Then and now: some comments on the design and analysis of slopes and embankments." *Proc. of Advances in Geotech Engineering*, 241-290.

Yaalon, D. H., and Kalmar, D. (1984). "Extent and dynamics of cracking in a heavy clay soil with xeric moisture regime." *Proc. Sym. on water & solute movement in heavy clay soils*. ILRI, Netherlands.

Yu, Z., Stirling, R. A., Davie, C. T., and Eminue, O. (2020). BIONICS cracking data. Newcastle University. Dataset.

Yu, Z., Stirling, R., Glendinning, S., Hughes, P., Brooks, H. (2021). Data from BIONICS research embankment. Newcastle University. Dataset.

Zein el-Abedine, A., and Robinson, G. H. (1971). "A study on cracking in some vertisols of the